The TEG-4 Gravity Field Model

B. D. Tapley, M. C. Kim, S. R. Poole, M. K. Cheng, D. P. Chambers, and J. C. Ries
Center For Space Research, The University of Texas at Austin

Center for Space Research
The University of Texas at Austin

Corresponding Author:
D. P. Chambers
(chambers@csr.utexas.edu)

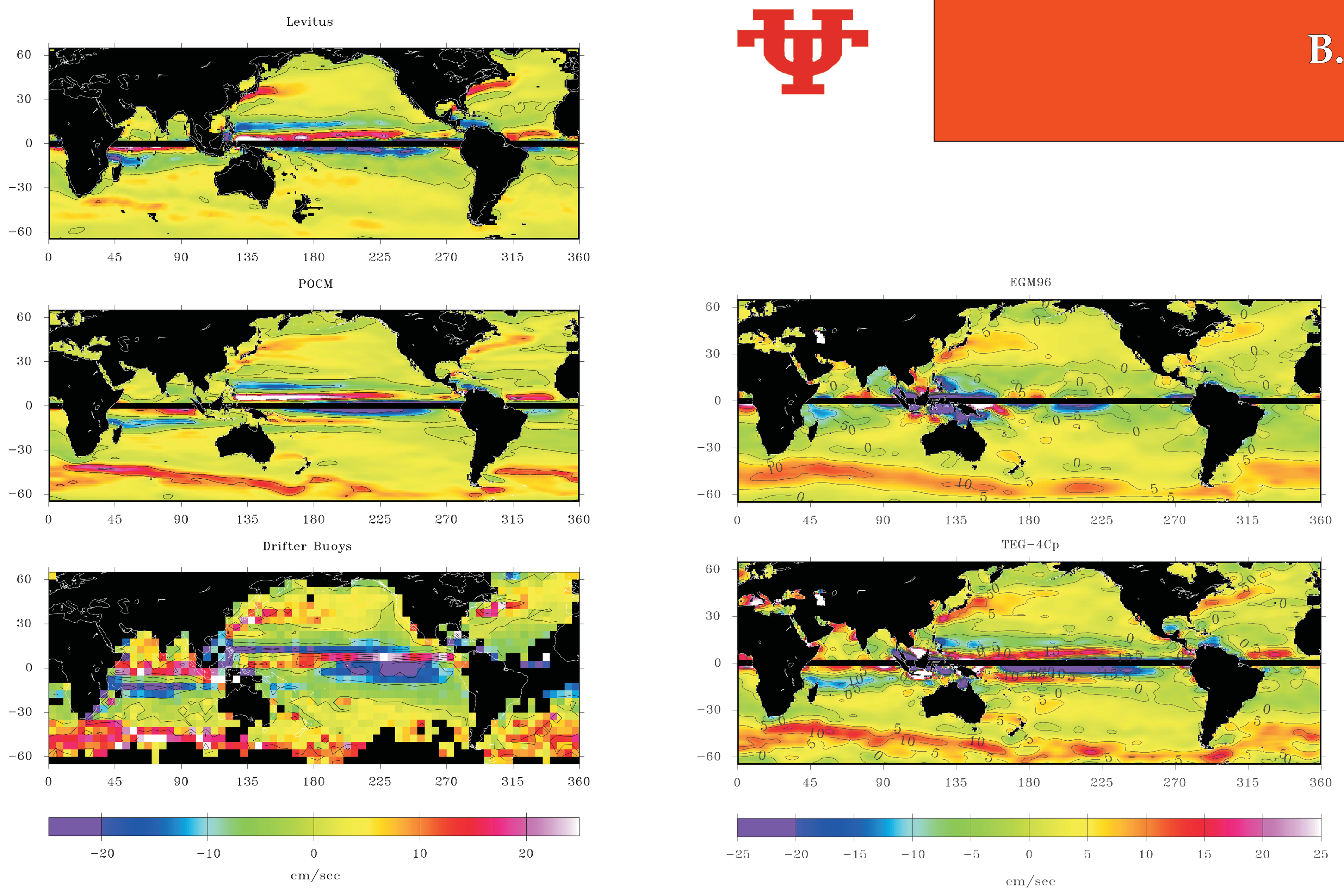

Figure 1. Zonal currents from Levitus and POCM DOT and drifter buoys (left) and T/P DOT with respect to geoid models (right). Eastward currents are positive.

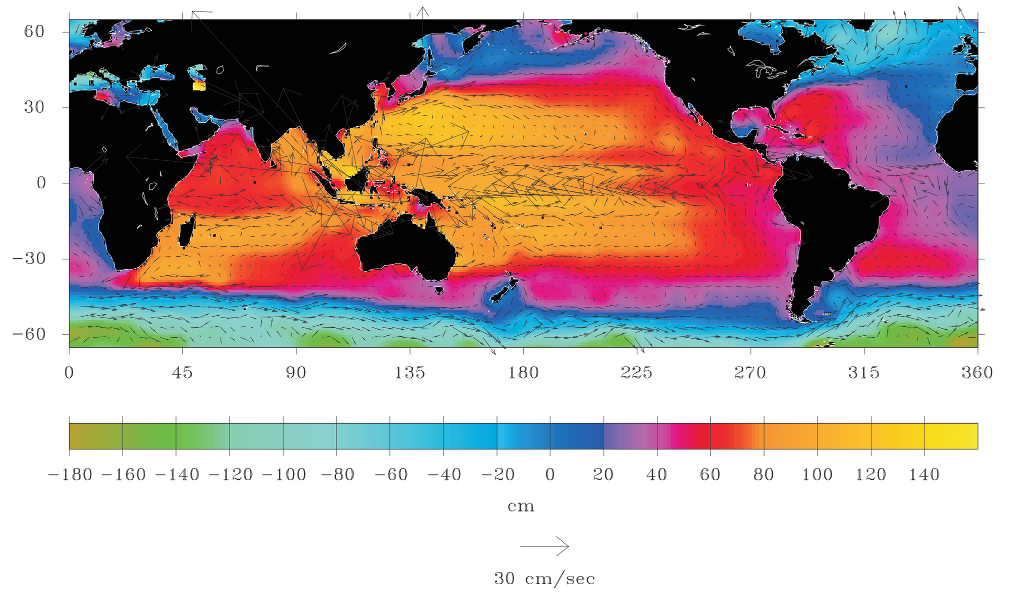

Figure 2. Dynamic ocean topography observed by T/P relative to the TEG-4Cp geoid. Vectors indicate size and direction of geostrophic currents.

Table 1. Data in TEG-4 solution, compared to TEG-3.

	TEG3		TEG4	
Data Set	**Data Span**	**Gravity Partials**	**Data Span**	**Gravity Partials**
Ajisai	1986-1991	34x34 + resonance	1993-1998	50x50 + resonance
BEC	1983-1986	28x28 + resonance	1/84-6/86	50x50 + resonance
DIC,DID,PEOLE	1971	34x34 + resonance	same	same
Etalon1	1989-1993	10x10	1989-1998	10x10
Etalon2	1989-1990	10x10	1989-1998	10x10
Geos3	255 days in 1980	40x40 + resonance	10/98-5/99	70x70 + resonance
Geosat	11/86-2/88 (Opnet)	34x34 + resonance	same	same
tracking	11/86-1/87 (Tranet)	"	same	same
altimeter	"	70x70	not in TEG4	
crossover	11/86-2/88 (Opnet)	70x70	same	same
Lageos1	1987-1993	20x20	1993-1998	20x20
Lageos2	10/92-8/93	20x20	1993-1998	20x20
Nova	95 days in 1984	36x36 + resonance	same	same
Oscar	72 days in 1980	36x36 + resonance	same	same
Spot2	1990	36x36 + resonance	1993-1998	70x70 + resonance
Spot2	1992	36x36 + resonance		
Starlette	1984-1992	50x50 + resonance	1993-1998	70x70 +resonance
Stella	9/93-2/95	34x34 + resonance	1993-1998	70x70 + resonance
TOPEX GPS	Cycles 10,15,17,19	34x34 + resonance	7/93-1/94	50x50 + resonance
TOPEX SLR and DORIS	10/3/92-5/9/93	36x36 + resonance	1993-1998	50x50 + resonance
ERS-1	5/94-9/94	34x34 + resonance	Not in TEG4	
ERS-1 slr	cycle 03	45x45 + resonance	same	same
ERS-1 slr	cycle 10	"	same	same
ERS-1 slr	cycle 16	"	same	same
ERS-1 alt	cycle 03	"	Not in TEG4	
ERS-1 alt	cycle 10	"	Not in TEG4	
ERS-1 alt	cycle 16	"	Not in TEG4	
GPSMET	6/19/95-7/9/95	36x36 + resonance	same	same
GFZ			6/95-12/97	70x70 + resonance
Westpac			8/98-7/99	70x70 + resonance
ERS-2 SLR			1997	45x45 + resonance
ERS-2 PRARE			1997	45x45 + resonance
Surface Gravity Anomaly		70x70		180x180
Marine Geoid				
Undulation				180x180

Table 2. Tracking data residual RMS when orbits are computed with various gravity field models.

	Gravity Model					
Tracking	**JGM-3**	**EGM96**	**TEG-3**	**GRIM5S1**	**TEG-4Sp**	**TEG-4Cp**
GEOS-3 SLR	7.9	8.3	7.9	9.5	6.7	8.7
ERS-1 SLR	6.8	6.1	3.6	4.0	4.9	3.7
ERS-2 SLR	6.8	6.8	3.3	3.7	3.2	3.7
ERS-2 PRARE (D)	0.67	0.66	0.59	0.57	0.57	0.63
ERS-2 PRARE (R)	7.9	7.0	6.0	5.4	5.4	7.0
ERS-2 XOVER	8.4	7.9	7.4	6.6	6.8	8.0
GFO SLR	12.2	12.0	12.0	15.8	17.1	11.3
LAGEOS-1,2 SLR	2.5, 2.5	2.5, 2.5	2.4, 2.4	3.0, 2.6	2.4, 2.5	2.4, 2.4
AJISAI SLR	5.2 (3.5)	5.3 (3.5)	5.6 (3.5)	4.9 (3.5)	4.7 (3.3)	5.5 (3.4)
STARLETTE SLR	7.2 (4.3)	6.4 (3.7)	6.7 (3.8)	6.3 (3.2)	6.5 (2.9)	6.5 (3.8)
STELLA SLR	9.3 (6.5)	8.8 (6.4)	5.6 (3.0)	5.9 (2.8)	5.0 (2.7)	5.2 (3.7)
WESTPAC SLR	7.5 (4.6)	10.3 (6.6)	8.0 (6.1)	10.2 (6.1)	8.8 (5.8)	10.5 (6.8)
GFZ-1	79.1 (40.8)	55.2 (36.7)	72.4 (37.9)	267.1 (24.6)	46.7 (26.9)	61.4 (32.2)
TOPEX SLR	2.3	2.4	2.3	2.0	2.0	2.2
TOPEX DORIS	0.54	0.54	0.54	0.54	0.54	0.54
TOPEX XOVER	6.1	6.2	6.1	6.0	6.1	6.1

Notes:
1) SLR, PRARE (Range) and altimeter XOVER residuals in cm.
2) PRARE (Doppler), TRANET, and DORIS residuals in mm/s.
3) For satellites with two values, the first value is for orbit estimated without 1 cpr parameters, the () value is for orbit estimated with 1 cpr parameters.
4) All evaluations used a tide model based on CSR 3.0.

Abstract

A new gravity field model complete to degree and order 180 has been computed. The model incorporates an improved reference frame and new SLR and DORIS tracking data for 13 satellites, including Lageos I and II, Etalon I and II, Starlette, Stella, Ajisai, BEC, Geos-3, GFZ, SPOT-2, TOPEX and Westpac, and 20 Cycles GPS data for TOPEX, and SLR and PRARE data from ERS-2. Surface gravity anomaly data and satellite altimeter-derived marine geoid undulations have also been included. The gravity field coefficients were allowed to adjust to the gravity information from altimetry after removing a reference topography derived from a contemporary ocean circulation model. The data have been combined with various weights, and the effect of relative data weighting on the solution has been investigated. The result of the study is a new high resolution gravity field that improves the determination of the general ocean circulation from satellite altimetry while maintaining or improving satellite orbit accuracies comparable to those obtained with older models.

Introduction

The results of this study are the latest in a series of Texas Earth Gravity (TEG) models. The previous model, TEG-3 [*Tapley et al.*, 1997] was computed by combining satellite tracking, altimetry, and surface gravity data in a joint solution and simultaneously estimating the spherical harmonic coefficients of the gravity field and dynamic ocean topography (DOT). The differences in the new TEG-4 models are:

- New satellite tracking with higher degree and order partials (Table 1).
- Complete to degree and order 180.
- An a priori DOT model based on output from a General Ocean Circulation Model (GOCM).
- An innovative, faster method to compute normal equations from surface geodetic data [*Kim and Tapley*, 1999].
- Altimetry data via a global mean sea surface (MSS) model computed from TOPEX/Poseidon (T/P), ERS-1, ERS-2, and Geosat data.
- DOT coefficients were not estimated simultaneously; this enabled the altimeter data to adjust the long wavelength components of the gravity field.

This poster presents results from two preliminary TEG-4 models, a satellite-only version designated TEG-4Sp, which is complete to degree and order 70, and a combined version, designated TEG-4Cp, which is complete to degree and order 180. We will discuss evaluations of the TEG-4 models compared to other recent models in terms of orbit comparison tests and comparison of recovered ocean circulation from altimetry with hydrographic data and model output.

Orbit Comparisons

The orbit fits relative to several gravity field models are given in Table 2. Many of the tests were performed with and without the estimation of one-cycle-per-revolution (1-cpr) empirical accelerations. These empirical accelerations are generally employed to remove, to a large degree, the effect of surface force modeling errors, but they also have the result of removing the secular and long-period orbit errors due to the even and odd zonals. Consequently, the tests without 1-cpr parameters reflect the effect of the zonal errors, whereas the tests with 1-cpr parameters evaluate the gravity model without the dominant effect of the zonal errors.

The satellite orbit tests must always be evaluated with caution. The arc lengths and estimated parameters for each case were designed to reduce the contribution of surface forces while avoiding excessive parameterization, but the choice is highly subjective. The GFZ-1 satellite, in particular, is strongly perturbed by atmospheric drag at its low altitude (400 km), and the SLR tracking is sparse, so these evaluations can differ considerably from tests conducted by others. In addition, all the tests were conducted with an ocean tide model based on the CSR 3.0 model, which may tend to bias the results slightly in favor of models produced by CSR. Some conclusions, however, can be drawn. For many satellites, all the models perform comparably, and improvements in their fits are increasingly difficult. No one model appears to be able to fit all the satellites best. Finally, it does appear that is still possible to obtain some improvement in the marine geoid as well as in the overall orbit fits beyond the models currently available.

Marine Geoid and Ocean Circulation

There is more differentiation between the models in the marine geoid and the dynamic ocean topography. The performance of the marine geoid is evaluated by comparing geostrophic currents computed relative to geoid models (such as JGM-3 [*Tapley et al.*, 1996] and EGM96 [*Lemoine et al.*, 1998]) as well as currents determined from the *Levitus* [1982] data and Parallel Ocean Climate Model (POCM) [*Semtner and Chervin*, 1992]. We have also examined ocean currents derived from drifter buoys, at a 5° resolution [*NOAA Atlantic Oceanographic and Meteorological Laboratory*].

It has already been noted that the DOT computed relative to the JGM-3 geoid model does not accurately reproduce the circulation of the tropics [*Stammer and Wunsch*, 1994; *Tapley et al.*, 1994]. The GRIM5S1 model [R. Biancale, personal communication, 1999] is not examined because it is a satellite only solution, and so will not have an adequate marine geoid.

The dynamic ocean topography is computed by differencing the marine geoid defined by each of the models from the CSRMSS95 [*Kim et al.*, 1995] mean sea surface model, corrected for the standard inverted barometer correction. The resulting DOT is then averaged to a 1° grid, and smoothed over long-wavelengths with a rectangular gaussian filter [*Chambers et al.*, 1997]. The geostrophic currents are computed from the dynamic topography except within ± 2° of the equator, where the Coriolis parameter approaches zero. The currents were computed in the same manner from 1° grids of POCM and *Levitus* [1982].

Since the POCM DOT was used as the a priori DOT in the TEG-4 solutions, the comparisons with the *Levitus* [1982] hydrography should give more conservative estimates of the error in TEG-4.

Figure 1 shows the zonal velocities from the altimeter DOT, POCM and Levitus DOT, and drifter buoys. Meridional velocities are not shown because they are smaller, and the zonal maps more clearly show changes in the equatorial regions. The maps from the Levitus and POCM DOT and the drifter buoys all show similar features: the Kuroshio extension, the Gulf Stream, the zonal currents and countercurrents in the tropics, and the Antarctic Circumpolar Current (ACC).

The speed of the ACC from the Levitus DOT is significantly slower than in the other maps due to the lack of data in the southern hemisphere. Also, there is a fairly strong countercurrent south of the equator in the Pacific in the POCM data that does not appear in the other maps. The currents from the drifter buoys tend to be larger than the currents in the DOT models, because the buoys are biased toward the strongest current and because the buoys measure the total current and not just the geostrophic component.

The maps from the altimetry data relative to EGM96 show a slightly weaker Kuroshio and Gulf Stream, but a similar ACC to the in situ and POCM data. The maps for JGM-3 and TEG-3 are qualitatively similar. In the tropics the differences are much larger. First, there is no sign of the Indian Ocean South Equatorial Countercurrent (SECC), or the Atlantic North Equatorial Countercurrent (NECC) and South Equatorial Current (SEC). Although the EGM96 map shows some evidence of the Pacific North Equatorial Current (NEC), it is pushed northward from where it appears in the in situ data and POCM, and it is weaker. Most importantly, none of the geoids (EGM96, JGM-3, or TEG-3) DOT show much evidence of the Pacific NECC.

The topography relative to TEG-4Cp produces better zonal currents in the tropics (Figure 1, Figure 2). The strength and locations of the tropical currents agree better with the in situ data and POCM for the TEG-4Cp DOT than for the JGM-3, EGM96, or TEG-3 DOT. For the first time, countercurrents appear in the Indian Ocean and the Atlantic. The Pacific NEC is in the proper position, with the strongest currents in the western portion of the basin.

There are some residual large and apparently erroneous signals around Indonesia in TEG-4Cp. We have traced this to a problem in the error values applied to the a priori DOT used in the solution. We are in the process of correcting this, and expect significant improvements in this area in the final TEG-4 model.

The standard deviation (σ) and correlation (ρ) of velocity components for all the altimetric DOTs relative to POCM, *Levitus* [1982] are given in Table 3. For comparison, the values differencing POCM and *Levitus* [1982] are also given.

Conclusions

The TEG-4Cp gravity model produces a better marine geoid than previous models in terms of recovering the long-wavelength ocean circulation. In particular, the TEG-4Cp model produces better zonal circulation in the tropics, which has been a problem in previous models. At the same time, the TEG-4Cp model produces orbits as well as or better than previous models, although not as good as the satellite only portion, TEG-4Sp.

Clearly, it is a challenging task to obtain significant improvement in the geopotential model with existing data. We look forward to the prospect of obtaining global and high precision gravity information from future space-geodetic missions such as CHAMP, GRACE, and GOCE.

References

Kim, M. C. and B. D. Tapley, Formation of surface spherical harmonic normal matrices and application to high degree geopotential modeling, J. of Geodesy, in review, 1999.

Lemoine, F. G., et al., The development of the joint NASA GSFC and NIMA geopotential model EGM96, *NASA TM-1998-206861*, 1998.

Levitus, S., Climatological atlas of the world ocean, *NOAA Prof. Pap. 13*, U. S. Govt. Print. Off. Washington, D.C., 1982.

Semtner, A. J., and R. M. Chervin, Ocean general circulation from a global eddy-resolving model, *J. Geophys. Res., 97*, 15502-15522 and 15767-15775, 1988,

Stammer, D. and C. Wunsch, Preliminary assessment of the accuracy and precision of the TOPEX/POSEIDON altimeter with respect to the large-scale ocean circulation, *J. Geophys. Res., 99*, 24584-24604, 1994.

Tapley, B. D., D. P. Chambers, C. K. Shum, R. J. Eanes, J. C. Ries, and R. H. Stewart, Accuracy assessment of the large-scale dynamic ocean topography from TOPEX/POSEIDON altimetry, *J. Geophys. Res., 99*, 24605-24617, 1994.

Tapley, B. D., et al., The joint gravity model 3, *J. Geophys. Res., 101*, 28029-28049, 1996.

Tapley, B. D., et al., The TEG-3 geopotential model, *Gravity, Geoid, and Marine Geodesy*, J. Seagwa, H. Fujimoto, and S. Okubo (Ed.), Springer-Verlag, 453-460, 1997.

Table 3. Statistics of velocity comparisons.

	Zonal		Meridional	
Comparison	**σ**	**ρ**	**σ**	**ρ**
JGM-3/Levitus	12.3	0.11	8.9	0.10
JGM-3/POCM	14.4	0.14	10.1	0.13
JGM-3/Buoy	14.9	0.16	----	----
EGM96/Levitus	6.7	0.31	3.7	0.33
EGM96/POCM	7.4	0.35	4.2	0.28
EGM96/Buoy	10.3	0.35	----	----
TEG-3/Levitus	11.5	0.11	8.2	0.09
TEG-3/POCM	13.4	0.14	9.2	0.13
TEG-3/Buoy	14.8	0.17	----	----
TEG-4Cp/Levitus	4.9	0.69	3.4	0.28
TEG-4Cp/POCM	6.4	0.64	4.9	0.32
TEG-4Cp/Buoy	9.0	0.54	----	----
POCM/Levitus	4.1	0.75	2.0	0.56

σ is standard deviation in cm/sec
ρ is correlation.